www.ietdl.org

Published in IET Intelligent Transport Systems
Received on 10th April 2014
Revised on 16th June 2014
Accepted on 1st July 2014
doi: 10.1049/iet-its.2014.0075

Special Section: 20th ITS World Congress, Tokyo 2013

ISSN 1751-956X

Fuzzy-based blended control for the energy management of a parallel plug-in hybrid electric vehicle

Nicolas Denis[1], *Maxime R. Dubois*[2], *Alain Desrochers*[3]

[1]*Smart Vehicle Research Center Laboratory, Toyota Technological Institute, 2-12-1, Hisakata, Tenpaku Ward, Nagoya, Japan*
[2]*Electrical and Computer Engineering Department, Sherbrooke University, 2500 Boulevard Université, Sherbrooke, Canada*
[3]*Mechanical Engineering Department, Sherbrooke University, 2500 Boulevard Université, Sherbrooke, Canada*
E-mail: nicolas.denis@toyota-ti.ac.jp

Abstract: The growing interest in reducing fuel consumption and gas emissions provides an incentive for the automotive industry to innovate in the field of hybrid electric vehicles (HEV) and plug-in hybrid electric vehicles (PHEV). The two embedded power sources in these vehicles require an intelligent controller in order to make the best decision on the power distribution. Actually these controllers, often called energy management systems, are very important and greatly influence the achievable fuel economy. Compared with an HEV, a PHEV allows battery discharge over a complete trip. As a consequence the optimal control of a PHEV implies a stronger dependence on the total driving cycle. Many authors have studied the possibility of fuzzy-based systems for both HEV and PHEV as they have proved to be robust, reliable and simple. However, classical fuzzy rule-based strategies demonstrate a lack of optimality because their design is focused on the actual vehicle state rather than the driving conditions. This study proposes a blended control strategy based on fuzzy logic for a PHEV. The proposed controller is fed with driving condition information in order to increase the controller effectiveness in every situation. The efficiency of the proposed controller is demonstrated through simulations.

1 Introduction

Hybrid electric vehicles (HEV) and plug-in hybrid electric vehicles (PHEV) are one of the most promising solutions to reduce the environmental impact of individual transportation. In a parallel hybrid configuration, the motoring shaft is shared by an internal combustion engine (ICE) and an electric motor. The intrinsic architecture of a parallel HEV or PHEV requires the implementation of an energy management system (EMS) that will determine the power split distribution effectively between the engine and the electric motor. A very important purpose of the EMS is to guarantee that the battery state of charge (SOC) is kept within an acceptable range while improving the fuel economy over a complete trip.

The state of the art in this field proposes many solutions that have their own advantages and drawbacks. For both HEV and PHEV, the literature roughly classifies the different control strategies into two categories which are 'rule-based strategies' and 'optimisation-based strategies' [1]. The rule-based strategies are subdivided into deterministic rule-based [2–6] and fuzzy rule-based methods. The optimisation-based strategies are based on a mathematical formulation of the energy management problem. In particular, global optimisation techniques allow finding the optimal power split value for each time of a predefined driving cycle. Such an optimisation problem is likely to be non-linear and constrained and consequently dynamic programming (DP) is a good candidate for solving the problem [7, 8]. Nevertheless, the strong computational complexity of DP is a significant drawback for a real-time application. Consequently, some authors proposed convex optimisation that requires much lower computational intensity [9]. However, all the parts of the vehicle powertrain have to be modelled by quadratic or linear functions for the convex optimisation to be performed. Equivalent consumption minimisation strategies (ECMS) are local optimisation by nature and therefore need less computation time compared with DP. It is primarily based on the heuristic that electrical energy can be expressed as an equivalent fuel quantity by introducing an equivalence factor. Some authors proposed to use ECMS for real-time applications [10, 11] and observed that fuel minimisation and final SOC boundary condition can be achieved by a careful adjustment of the equivalence factor that strongly depends on the whole driving cycle. Moreover, some authors used Pontryagyn's minimum principle (PMP) to perform global optimisation [12] and showed the close mathematical relation between the costate of the PMP problem and the equivalence factor of the ECMS. They also

showed that under assumptions on the battery behaviour, a single constant value for the equivalence factor can lead to fuel consumption very close to the achievable minimum. Nevertheless, the optimal value depends on the driving cycle.

Fuzzy rule-based strategies have proven to increase the vehicle performance compared with the deterministic rule-based strategies [13]. Simple fuzzy rule-based strategies have been proposed by several authors [14–20]. They aim at controlling the SOC while favouring efficient operation of the powertrain. The SOC is the primary input and is combined with other vehicle inputs such as the required torque, required power, vehicle speed, vehicle acceleration, motor speed and ICE speed. This kind of approach offers computational simplicity but requires human expertise and a 'trial and error' process that lead to non-optimal performances. It is nonetheless possible to reduce human impact by adopting optimisation techniques directly on fuzzy systems. One solution is to intelligently choose the fuzzy rules by the straightforward observation of off-line computed DP results [21]. Genetic algorithms have also been investigated for the optimisation of the membership functions of the fuzzy-logic controller [22–24]. A similar approach consists in using an adaptive neural fuzzy inference system to optimise fuzzy memberships and rules [25] with a neural network that needs previously computed optimal control sequence on a predefined driving cycle for neural network training. Optimisation of fuzzy rules is performed off-line on predefined driving cycles. The resulting fuzzy logic controller then offers quasi-optimal performance on the considered driving cycles but may remain non-optimal for other speed profiles. Consequently some authors propose to combine optimised fuzzy rule-based strategies with real-time driving style recognition [26] or driving condition recognition [27–29]. The driving style recognition aims at estimating the driver's behaviour on the acceleration pedal while the driving condition recognition is responsible for the road type (urban, arterial, highway) and traffic level estimation. The obtained controllers are then usable in real-time and have the ability to adapt themselves to the current driving scenario.

A significant difference exists between the power split management of an HEV and that of a PHEV with respect to their SOC. Since the battery of an HEV cannot be charged through an external plug, its EMS uses a charge sustaining (CS) strategy in order to maintain the SOC around a constant value. On the contrary, a PHEV will benefit from an external plug and will be charged during its off state. Hence, in a PHEV, the end-of-trip SOC will be lower than its initial SOC. The question remains, as to how fast should the battery depletion occur? Global optimisation shows that whenever the all-electric range (AER) of a PHEV is exceeded, a blended battery depletion strategy is preferred where the ICE and the electric motor are used together before the low SOC level is reached. Fuzzy-based strategies for the control of a PHEV usually deplete the battery by making the vehicle work like an electric vehicle (EV) during the first part of the trip and then maintain the SOC to a constant level, much like an HEV [30, 31]. As a consequence, there is a motivation to propose a fuzzy-based blended control strategy as it can lead to a compromise between computational simplicity, real-time use and fuel minimisation.

This paper proposes a fuzzy-based EMS that is able to perform a blended strategy by using past and current driving information together with the expected trip distance in an original manner. Moreover an original way of optimising fuzzy characteristics by using DP is proposed and the results show that our controller remains simple and reliable while the use of driving information allows an adaptive control relative to the different driving conditions. Section 2 will present the powertrain topology, Section 3 will describe the analyse of the optimal control of the vehicle provided by DP on several driving cycles, Section 4 will present the developed real-time controller and finally Section 5 will expose the simulation results.

2 Description of the vehicle

The vehicle described in this paper is a three-wheel roadster that already exists in its conventional form (with only an ICE). In order to reduce its fuel consumption without sacrificing its autonomy, it has been proposed to develop a plug-in hybrid form of this vehicle. The challenge is therefore to modify the complete powertrain without altering the vehicle design too much. The constraints of space are a major concern and they greatly influenced the choices made for the powertrain architecture. A schematic of the vehicle is provided in Fig. 1. A parallel topology has been chosen because a preliminary study has proved that this topology would take less space than a series architecture. The specific geometry of the vehicle requires a primary and secondary drive for the disposition of the powertrain components. The battery pack can be regenerated by electrically braking the vehicle or by overpowering the engine. In all cases, the power contributions from the two power sources have to satisfy the driver's demand. The torque and speed equations can be written as

$$N_{\mathrm{w}} = \frac{N_{\mathrm{ICE}}}{i_{\mathrm{pr}}.i_{gb}(k).i_{\mathrm{sec}}.i_{\mathrm{fin}}} = \frac{N_{\mathrm{e}}}{i_{\mathrm{mg}}.i_{\mathrm{fin}}} \tag{1}$$

(see (2))

where N_{w}, N_{ICE} and N_{e} are, respectively, wheel, engine and motor speeds, T_{w}, T_{ICE} and T_{e} are, respectively, wheel, engine and motor torques, i_{pr}, i_{sec}, i_{mg} and i_{fin} are, respectively, primary, secondary, motor and final drive ratio, i_{gb} is the gear ratio of the gearbox which depends on the selected gear number k. The gearbox is composed of six different gears. η_{pr}, η_{sec}, η_{mg}, η_{gb} and η_{fin} are the drive efficiencies, P_{w}, P_{e} and P_{ICE} are wheel, motor and engine mechanical power and sg is the sign function.

The electrical powertrain is composed of a battery pack that provides power to a voltage source inverter using IGBTs, the latter being able to drive a permanent magnet synchronous motor (PMSM). For a matter of space in our vehicle, two major choices were made. The electrical powertrain does not include a DC/DC converter in order to stabilise the bus voltage. Consequently, the inverter sees a variable bus voltage depending on the required battery current. This affects the whole electrical powertrain efficiency. Moreover

$$\frac{T_{\mathrm{w}}}{i_{\mathrm{fin}}}\left(\frac{1-sg(P_{\mathrm{w}})}{2}\eta_{\mathrm{fin}} + \frac{1+sg(P_{\mathrm{w}})}{2}\frac{1}{\eta_{\mathrm{fin}}}\right) = T_{\mathrm{ICE}}.\, i_{\mathrm{pr}}.i_{gb}(k).i_{\mathrm{sec}}.\eta_{\mathrm{pr}}.\eta_{gb}.\eta_{\mathrm{sec}} + T_{\mathrm{e}}.i_{\mathrm{mg}}\left(\frac{1-sg(P_{\mathrm{e}})}{2}\frac{1}{\eta_{\mathrm{mg}}} + \frac{1+sg(P_{\mathrm{e}})}{2}\eta_{\mathrm{mg}}\right) \tag{2}$$

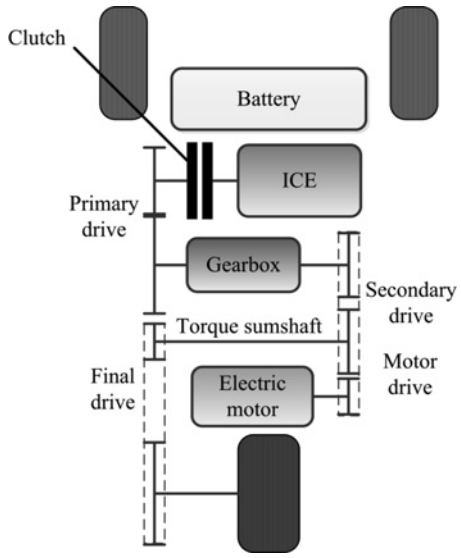

Fig. 1 *Schematic of the parallel plug-in hybrid electric roadster*

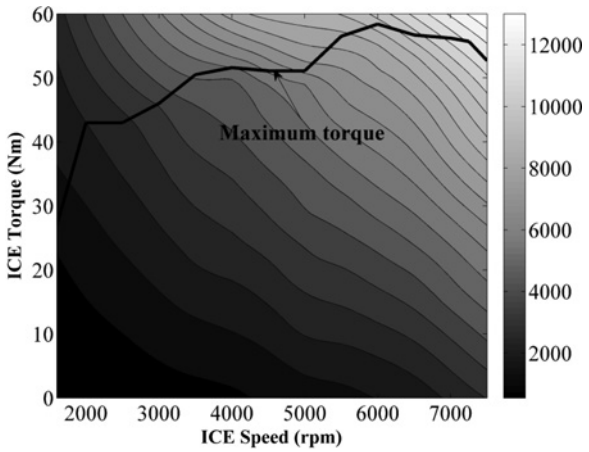

Fig. 2 *ICE instantaneous consumption (g/h)*

there is no clutch on the electric motor shaft which means that the electric motor is always coupled to the wheel.

The complete vehicle model was established in a previous work [32], the mechanical model provides an estimation of the required torque based on the information of the vehicle speed, the engine is simulated using a map illustrated in Fig. 2 that provides instantaneous consumption for every speed and torque and finally the electrical powertrain was characterised by its mathematical equations. The vehicle specifications are provided in Table 1. The smallness of the battery pack is caused by the reduced available space in the vehicle. The battery is composed of Li-Ion cells A123 ANR26650m1A which are modelled by a variable voltage source in series with an internal resistance. The open circuit voltage value depends mainly of the cell SOC and follows the equation that can be found in [33]. The internal resistance value has been characterised regarding the cell temperature, current and SOC following the experimental protocol described in [34]. Finally, some other correction parameters proposed in [35] have been added in order to account for cell terminal voltage and state of discharge variations with cell current and temperature. Even if this model is simple and accurate enough for the purpose of the vehicle simulation, a more accurate first order RC model could have been used instead [36].

3 Analysis of the optimal vehicle behaviour

3.1 Dynamic programming algorithm

Since DP is a well-known tool that has been often used in literature for the problem of energy management of HEV and PHEV, this paper will not explain the DP theory in detail. A mathematical explanation of the DP algorithm can be found in [37]. In our case, DP has been used to find the optimal values of the ICE torque T_{ICE} and the gear number k that minimise the global fuel consumption over a complete driving cycle. For each time of a given driving

Table 1 Vehicle specifications

ICE		4 strokes – 2 cylinders	
		engine displacement	600 cm^3
		idle speed	1600 rpm
PMSM		maximum speed	8000 rpm
		number of pole pairs	5
		d-axis inductance	90 μH
		q-axis inductance	90 μH
		stator windings resistance	15 mΩ
		magnet flux amplitude	0.0543 Wb
Inverter	IGBT	rated collector current	550 A
		rated On-state collector-emitter voltage	1.35 V
		threshold voltage	0.8 V
	Diode	rated forward current	550 A
		rated forward voltage	1.35 V
		threshold voltage	0.9 V
Battery		embeddable energy	2.5 kWh
		rated output voltage	363 V
		cell capacity	2.3 Ah
Vehicle dynamics		weight	565 kg
		drag coefficient	0.537
		frontal area	1.19 m^2
		first order rolling resistance coefficient	0.0155
		second order rolling resistance coefficient	7.93×10^{-4} s/m
		third order rolling resistance coefficient	3.17×10^{-6} s^2/m^2
Vehicle geometry		length	2667 mm
		width	1506 mm
		height	1145 mm
		wheel base	1714 mm
		ground clearance	115 mm

doi: 10.1049/iet-its.2014.0075

cycle, the electric motor torque T_{EM} can be found from (2) knowing the optimal values of T_{ICE} and k. The optimal values of T_{ICE} and k are chosen within a range defined by their respective constraints.

Finally, an arbitrary value between 30 and 95% is imposed for the initial SOC and since the goal is to minimise the fuel consumption, the final SOC is imposed at 30%. It is considered that the degradation of the battery is accelerated when the SOC is under 30%. However DP allows the SOC to temporarily evolve between 20 and 30% during a driving cycle. A SOC above 95% or under 20% is not allowed by DP.

3.2 Dynamic programming results analysis

Since DP requires long computation and also the precise knowledge of the future driving cycle, it cannot be used directly in real-time hence it was decided to run it offline on the 11 Facility-Specific Drive Cycles developed by Sierra Research Inc. [27] which describe vehicle operation over different types of roadway (arterial, local and freeway) with several facility and traffic levels, called level of service (LOS).

The purpose of this offline DP solving was to observe the optimal behaviour coming from the DP results in order to build embeddable control laws that will mimic this optimal behaviour. Since there is no clutch on the electrical powertrain, the vehicle can be run in only two main modes which are pure electric or hybrid. Also, the purpose of the DP results observation is to try to establish two laws

- Law 1 is responsible for the power split decision during hybrid mode.
- Law 2 is responsible for the transition between pure electric and hybrid mode.

As an example, this section provides the results obtained after the DP algorithm was run on the arterial roadway with LOS A-B (ART LOS A-B) which corresponds to the lowest traffic and facility level for an arterial roadway. The initial SOC was imposed at a level of 50% in order to be able to observe a significant portion of hybrid operation. DP results will be different for another vehicle but the proposed methodology remains applicable to all cases.

To deal with the first law, the optimal engine load points coming from the DP results were plotted for every speed cycles. Fig. 3 shows this plot for the example of ART LOS A-B. Each red dot represents an operating point as issued from the DP optimisation sequence. In each speed cycle, it was observed that the engine should always work around its maximum efficiency in hybrid mode.

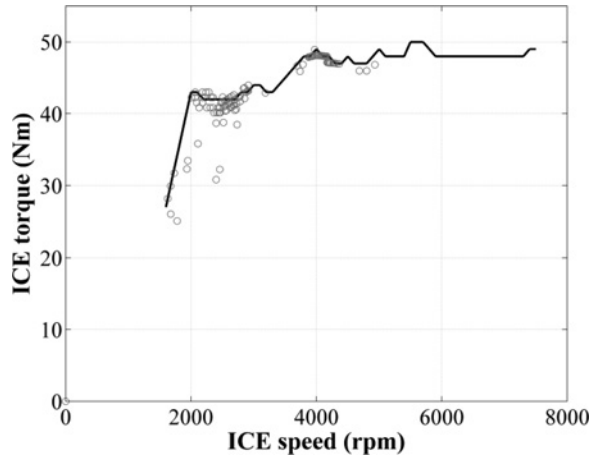

Fig. 3 *Optimal ICE loads points (circles) and maximum efficiency curve (solid line) on ART LOS A-B*

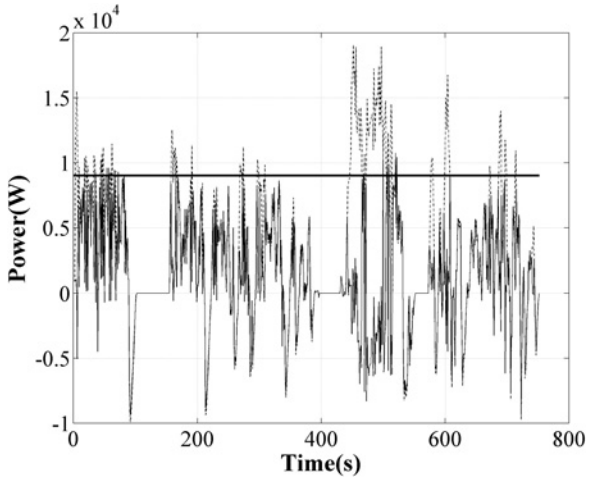

Fig. 4 *Comparison on ART LOS A-B between the required power (dashed curve) and the motor optimal power (solid curve)*
The power threshold is illustrated by the solid line

Now, the question remains as to when pure electric or hybrid modes should be selected. In order to visualise the optimal working mode chosen by DP, the required power to the wheel and the optimal electric motor power computed by DP were compared. Fig. 4 shows this comparison for the example of ART LOS A-B. The lines where the power of the electric motor matches the vehicle required power indicate that the optimal working mode is pure electric and the engine is turned off. On the contrary, hybrid is the optimal mode when the power from the electric motor is maintained below the vehicle required power. On Fig. 4, it can be observed that the hybrid mode is chosen by DP as soon as the required power is above a given power threshold P_{th}. In other words, when the vehicle required power is under a threshold P_{th}, the optimal working mode will be pure electric. This observation can actually be made on every driving cycles with different level of P_{th}. It will be the core of the mode transition management of the EMS controller.

The absence of a DC/DC converter between the battery and the inverter and the need for a flux weakening current at higher rotational speeds will increase the power losses in the whole electrical powertrain when high mechanical power is required. Examining the results from the DP optimisation of Fig. 4, this can explain why the electric motor operates in a relatively low range of power. More interestingly, the different results showed that the above mentioned power threshold can be observed for every speed cycle but varies with the type of driving pattern, the initial SOC and the length of the trip. Generally speaking, P_{th} increases for high speed cycles and decreases for low speed/urban cycles. At the same time, the power threshold will naturally increase for higher initial SOC in order to favour pure electric mode and battery discharge. The choice of a P_{th} value by simple observation of the DP results can be inaccurate hence a function f was introduced, expressed as

$$f(P_{th}) = \left|SOC_{tar} - SOC_f\right| \quad (3)$$

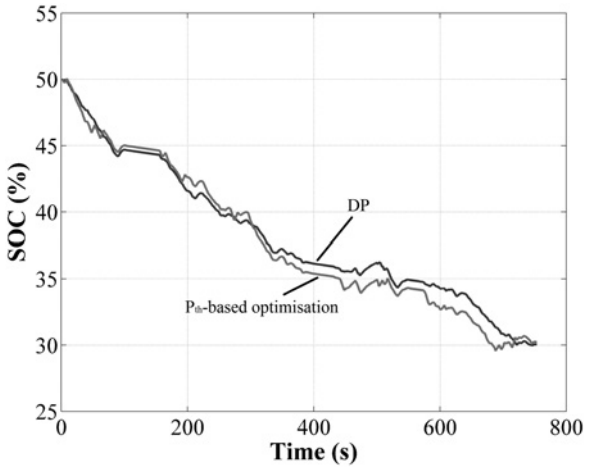

Fig. 5 *SOC comparison on ART LOS A-B between DP (black) and the P_{th}-based optimisation (grey)*

where SOC_{tar} is the targeted final SOC of 30% and SOC_f is the final SOC which will be obtained using a certain value of P_{th} on a given speed cycle. The aim will be to minimise f regarding P_{th}. As the function is strictly monotonic, it is possible to use a simple and fast binary search. The minimisation will assure a final SOC close to 30% and the intrinsic nature of the transition threshold P_{th} will assure a fuel consumption close to the achievable minimum. As an example, the optimal performances obtained with DP and the performances obtained using the proposed P_{th}-based optimisation were both compared on ART LOS A-B. The comparison on SOC evolution is illustrated in Fig. 5, a fuel consumption of 2.31 L/100 km was obtained with DP while the proposed optimisation yielded 2.47 L/100 km.

The function f will help in the design of the controller as will be shown in the next section.

4 Controller design

Firstly, in the light of the ICE load points observation illustrated in Fig. 3, the proposed controller will implement law 1 with the use of two 2D maps which will impose T_{ICE} and k in order to maximise the ICE efficiency for every possible vehicle speed and demanded torque.

These 2D maps form the hybrid mode of the controller. Whenever hybrid mode is chosen, the engine torque and gear number will be selected so as to maximise the ICE efficiency. The right power level should then be imposed to the electric motor in order to satisfy the torque requirement of the driver.

Law 2 will be implemented using the power threshold P_{th}. The vehicle will operate on hybrid or electric mode when the required power is, respectively, above or under P_{th}. In this case, the value of P_{th} will be computed using a fuzzy logic controller.

As the optimal power threshold depends on the driving conditions, the fuzzy logic controller should retain some form of driving pattern recognition. In this paper, three driving patterns are used, corresponding to 'Arterial LOS A-B', 'Freeway LOS A-C' and 'Freeway LOS G'. They cover a wide speed range and have very different speed distribution profiles. A histogram of vehicle velocity for the 3 speed cycles was plotted and approximated using Gaussian distributions. These distributions will be used to build the membership functions of the speed input for the fuzzy logic controller as will be shown later.

As presented earlier, the power threshold varies with the initial SOC and the total length of the trip. In order to reduce the complexity of the problem the 'global discharge rate' was introduced and defined by (4) as

$$\mathrm{dis}_{\mathrm{rate}} = \frac{\mathrm{SOC}_{\mathrm{init}} - \mathrm{SOC}_{\mathrm{tar}}}{l_t} \tag{4}$$

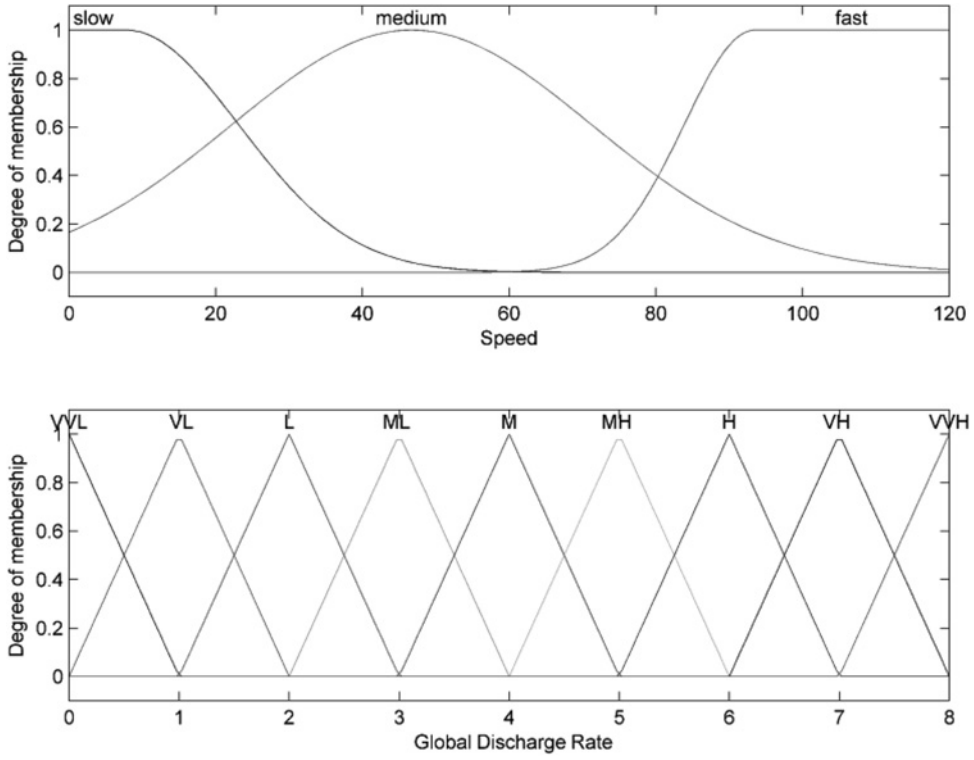

Fig. 6 *Membership functions for speed input (above) and global discharge rate input (under)*

doi: 10.1049/iet-its.2014.0075

where SOC_{init} is the initial SOC and l_t is the length of the trip. According to the above definition, the global discharge rate is expressed in %/km. For a given facility-specific driving cycle with a defined length, the global discharge rate will be determined by the initial SOC only. As explained in Section 3, the targeted final SOC is 30%. Consequently, the global discharge rate will increase with the initial SOC. Above a certain level, the AER of the vehicle will be reached and there will be no need for transition management anymore since it will be possible to make the whole trip using only the electric motor. Furthermore, it was found that the AER was reached above 4.80%/km for FW LOS G, 5.43%/km for ART LOS A-B and 7.93%/km for FW LOS A-C. Consequently there is an optimal P_{th} for each of the three driving cycles and for each values of global discharge rate between 0%/km (CS) and the maximum level that was previously determined. Finally, it was decided to find the optimal value of P_{th} by minimising f on each speed cycle and for the global discharge rate values 0 (VVL), 1, 2, …, 8%/km (VVH).

Based on this analysis, the fuzzy logic controller can be designed. It will have two inputs and one output, the first input being a moving average of the past speed. As it can be seen on Fig. 6, the membership functions for the speed are defined by the previous Gaussian distributions. The speed distribution for FW LOS A-C corresponds to the membership 'fast', the one for ART LOS A-B corresponds to 'medium' and the one for FW LOS G corresponds to 'slow'. This way, the fuzzy logic controller can locate current speed among the three speed distributions, and thus, benefit from the past driving information to adapt the control logic. The second input is the current global discharge rate. It is computed by dividing the difference between the current SOC and the targeted final SOC with the remaining distance. Using this input, the controller will, at any time of the trip, consider that the trip from the current time until the end time is a new trip with a given initial SOC. It will also assume that this new trip will follow the driving pattern that was detected by analysing the past data of the current trip. The memberships of the global discharge rate input can be seen on Fig. 6 and cover the range of discharge rate from 0 to 8%/km according to the previous analysis.

The fuzzy logic controller is a Sugeno-type and the output is the power threshold P_{th}. Each rule uses 'and' logic operators and imposes a suitable value of P_{th} depending on the inputs. An example of such rule would be

If Speed is 'medium' **and** GlobalDischargeRate is 'L' **then** P_{th} is 10 455 W.

Table 2 Fuzzy rules

Rate	Speed		
	Slow, W	Medium, W	Fast, W
VVL	3937	7684	7523
VL	5250	8655	10 457
L	6562	10 455	12 908
ML	7957	11 341	15 094
M	9680	13 728	17 106
MH	10 459	16 740	20 125
H	10 459	19 095	21 171
VH	10 459	19 095	23 556
VVH	10 459	19 095	32 157

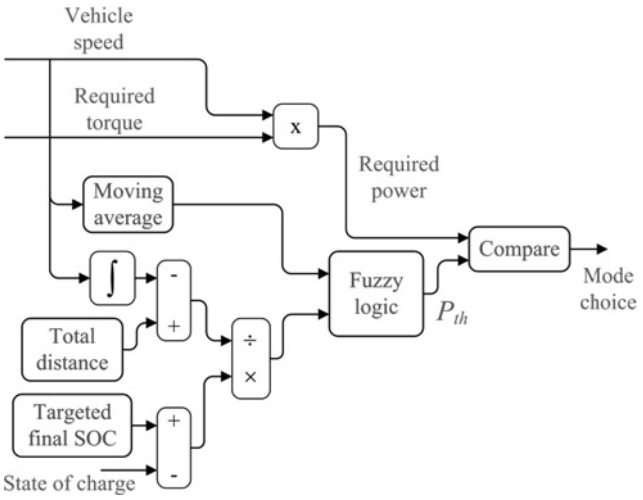

Fig. 7 *Embedded control logic for the mode transition management*

The values of P_{th} in the rules are selected based on the previous analysis using the minimisation of the function f. All the rules are presented in Table 2. According to the input values, membership degrees μ are computed for each fuzzy linguistic using the membership functions. Following the example above, the implied membership degrees would be μ_L for discharge rate and μ_{Medium} for speed. The computation of P_{th} requires the knowledge of the firing strengths w_j of all the rules. They are basically the weight factors to apply to each rule. The operator 'min' has been chosen as the inference method for the 'and' logic hence the firing strength of the example rule will be $w_j = \min(\mu_L, \mu_{Medium})$. The firing strength being defined for all the rules, the final power threshold will be computed using (5) as

$$P_{th} = \sum_{j=1}^{N_r} \frac{w_j P_{th,j}}{w_j} \quad (5)$$

with N_r the number of rules and $P_{th,j}$ the power threshold implied by the j^{th} rule.

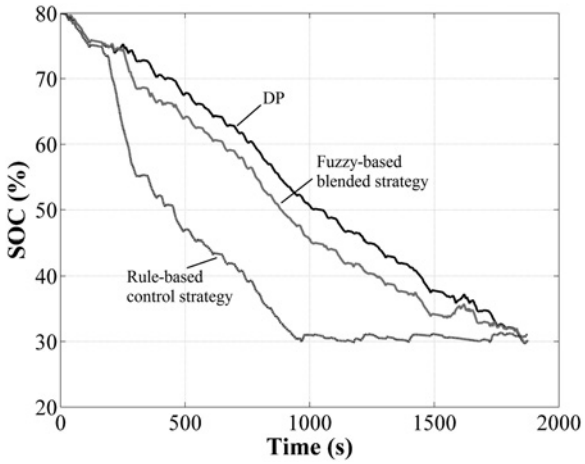

Fig. 8 *SOC comparison on UDDS between DP (black), fuzzy-based blended strategy (light grey) and rule-based control strategy (grey)*

Table 3 Fuel consumption comparison on different driving cycles

Driving cycle name	Initial SOC, %	DP, L/100 km	Fuzzy-based blended strategy	
			Final SOC, %	Fuel consumption, L/100 km
UDDS	80	1.89	30.1	2.01
HWFET	80	2.46	30.4	2.50
US06	80	3.44	32.2	3.54
NEDC	60	2.26	29.5	2.30

5 Simulation results

The proposed controller was integrated in the simulation tool as illustrated in Fig. 7. The speed moving average was made on the past 60 s. The computation of the current global discharge rate needed the feedback from the SOC and the total distance of the trip which can easily be retrieved from a GPS in a real-time application. The proposed real-time controller was tested on the urban dynamometer driving schedule (UDDS). Performances were compared with the DP control strategy and also the rule-based power follower strategy [3, 4]. The power follower does not have any previous knowledge of the trip and makes the vehicle run like an EV during the first part of the trip and later, enters the CS strategy where the ICE provides the most important part of the power while the SOC is maintained. Such a strategy is commonly called EVCS. The initial SOC was 80% for the three strategies and the SOC comparison can be seen in Fig. 8. A fuel consumption of 2.01 L/100 km was obtained for the fuzzy-based EMS while the DP algorithm showed a minimal consumption of 1.89 L/100 km and the rule-based strategy yielded a fuel consumption of 2.62 L/100 km. A fuel consumption comparison between DP and the proposed fuzzy-based blended strategy is available in Table 3. The comparison has been made for several driving cycles including UDDS. Using the fuzzy-based blended strategy allows to reach a final SOC which is close to the target of 30% but is not exactly 30%. Consequently, for the comparison of Table 3, the final SOC of DP was constrained to be equal to the final SOC obtained with the proposed fuzzy-based EMS. Since NEDC is a relatively short driving cycle, an initial SOC of 60% has been imposed for NEDC in order to obtain a meaningful result in terms of fuel economy.

6 Conclusion

Based on the DP results, a comprehensive methodology for the design of a real-time fuzzy-based EMS was proposed for a plug-in hybrid EV. The fuzzy-based EMS showed it was able to perform a blended discharge strategy, which is more suitable for a PHEV, by analysing the past speed of the current trip and adapting itself to the current driving pattern. The controller is easily embeddable and only needs the total length of the trip. It was able to reduce the fuel consumption over a classical rule-based strategy which does not benefit from trip information. A reduction of 27% in fuel consumption was observed with the proposed methodology on a UDDS driving profile. The proposed EMS also allows obtaining fuel consumption very close to the achievable minimum computed by DP for several normalised driving cycles. In case of an unknown trip length, the proposed strategy would be adapted to perform EV operation followed by a CS operation based on the proposed fuzzy control. In future works, it would be interesting to evaluate the impact on fuel economy when using such an adapted EVCS control strategy rather than the proposed blended strategy.

7 Acknowledgments

The authors wish to thank the BRP Corporation and Automotive Partnership Canada (APC) for supporting and funding this work.

8 References

1 Wirasingha, S.G., Emadi, A.: 'Classification and review of control strategies for plug-in hybrid electric vehicles', *IEEE Trans. Veh. Technol.*, 2011, **60**, (1), pp. 111–122
2 Phillips, A.M., Jankovic, M., Bailey, K.E.: 'Vehicle system controller design for a hybrid electric vehicle'. Proc. IEEE Int. Conf. on Control Applications, Anchorage, USA, September 2000, pp. 297–302
3 Ehsani, M., Gao, Y., Emadi, A.: 'Parallel (mechanically coupled) hybrid electric drive train design', in (Eds.): 'Modern electric, hybrid electric, and fuel cell vehicles' (CRC Press, 2010, 2nd edn.), pp. 283–295
4 Salmasi, F.R.: 'Control strategies for hybrid electric vehicles: evolution, classification, comparison, and future trends', *IEEE Trans. Veh. Technol.*, 2007, **56**, (5), pp. 2393–2404
5 Banvait, H., Anwar, S., Chen, Y.: 'A rule-based energy management strategy for plug-in hybrid electric vehicle (PHEV)'. Proc. ACC, St-Louis, USA, June 2009, pp. 3938–3943
6 Sun, L., Liang, R., Wang, Q.: 'The control strategy and system preferences of plug-in HEV'. Proc. VPPC, Harbin, China, September 2008, pp. 1–5
7 Yang, C., Li, J., Sun, W., Zhang, B., Gao, Y., Yin, X.: 'Study on global optimisation of plug-in hybrid electric vehicle energy management strategies'. Proc. APPEEC, Chengdu, China, March 2010, pp. 1–5
8 Karbowski, D., Rousseau, A., Pagerit, S., Sharer, P.: 'Plug-in vehicle control strategy: from global optimisation to real-time application'. Proc. EVS 22, Yokohama, Japan, October 2006, pp. 1–12
9 Hu, X., Murgovski, N., Johannesson, L., Egardt, B.: 'Energy efficiency analysis of a series plug-in hybrid electric bus with different energy management strategies and battery sizes', *Appl. Energy*, 2013, **111**, pp. 1001–1009
10 Tulpule, P., Marano, V., Rizzoni, G.: 'Energy management for plug-in hybrid electric vehicles using equivalent consumption minimisation strategy', *Int. J. Electr. Hybrid Veh.*, 2010, **2**, (4), pp. 329–350
11 Zhang, C., Vahidi, A.: 'Route preview in energy management of plug-in hybrid electric vehicles', *IEEE Trans. Control Syst. Technol.*, 2012, **20**, (2), pp. 546–553
12 Kim, N., Cha, S., Peng, H.: 'Optimal control of hybrid electric vehicles based on Pontryagin's minimum principle', *IEEE Trans. Control Syst. Technol.*, 2011, **19**, (5), pp. 1279–1287
13 Kahrobaeian, A., Asaei, B., Amiri, R.: 'Comparative investigation of charge-sustaining and fuzzy logic control strategies in parallel hybrid electric vehicles'. Proc. IEEE VPPC, Dearborn, USA, September 2009, pp. 1632–1636
14 Lu, D., Li, W., Xu, G., Zhou, M.: 'Fuzzy logic control approach to the energy management of parallel hybrid electric vehicles'. Proc. IEEE Int. Conf. on Information and Automation, Shenyang, China, June 2012, pp. 592–596
15 Anderson, T.A., Barkman, J.M., Mi, C.: 'Design and optimisation of a fuzzy-rule based hybrid electric vehicle controller'. Proc. IEEE VPPC, Harbin, China, September 2008, pp. 1–6
16 Majdi, L., Ghaffari, A., Fatehi, N.: 'Control strategy in hybrid electric vehicle using fuzzy logic controller'. Proc. IEEE Int. Conf. on Robotics and Biomimetics, Guilin, China, December 2009, pp. 842–847
17 Li, Q., Chen, W., Li, Y., Liu, S., Huang, J.: 'Energy management strategy for fuel cell/battery/ultracapacitor hybrid vehicle based on fuzzy logic', *Int. J. Electri. Power Energy Syst.*, 2012, **43**, pp. 514–525
18 Sarvestani, A.S., Safavi, A.A.: 'A novel optimal energy management strategy based on fuzzy logic for a hybrid electric vehicle'. Proc. ICVES, Pune, India, November 2009, pp. 141–145
19 Amiri, M., Esfahanian, V., Hairi-Yazdi, M.R., Esfahanian, M., Fazedi, A.M., Nabi, A.: 'Feed-forward modelling and fuzzy logic based control strategy for powertrain efficiency improvement in a parallel hybrid electric vehicle', *Math. Comput. Model. Dyn. Syst.*, 2009, **15**, (2), pp. 191–207

doi: 10.1049/iet-its.2014.0075

20 Yang, L., He, H., Sun, F., Shi, S., Li, Y., Liu, L.: 'Research of fuzzy logic control strategy for engine start/stop in dual-clutch hybrid electric vehicle'. Proc. FSKD, Yantai, China, August 2010, pp. 912–917

21 Chen, Z., Mi, C.C.: 'An adaptive online energy management controller for power-split HEV based on dynamic programming and fuzzy logic'. Proc. IEEE VPPC, Dearborn, USA, September 2009, pp. 335–339

22 Yang, S., Li, M., Weng, H., *et al*.: 'Research on genetic-fuzzy control strategy for parallel hybrid electric vehicle', *World Electr. Veh. J.*, 2011, **4**, (1), pp. 224–231

23 Zhou, M., Lu, D., Li, W., Xu, H.: 'Optimized fuzzy logic control strategy for parallel hybrid electric vehicle based on genetic algorithm', *Appl. Mech. Mater.*, 2013, **274**, pp. 345–349

24 Ravey, A., Blunier, B., Miraoui, A.: 'Control strategies for fuel-cell-based hybrid electric vehicles: from offline to online and experimental results', *IEEE Trans. Veh. Technol.*, 2012, **61**, (6), pp. 2452–2457

25 Meng, X., Langlois, N.: 'Optimized fuzzy logic control strategy of hybrid vehicles under different driving cycle'. Proc. CCCA, Hammamet, Tunisia, March 2011, pp. 1–6

26 Wang, Q., Tang, X., Sun, L.: 'Driving intention identification method for hybrid vehicles based on fuzzy logic inference'. Proc. FISITA World Automotive Congress, Beijing, China, November 2012, pp. 287–298

27 Langari, R., Won, J.-S.: 'Intelligent energy management agent for a parallel hybrid vehicle – Part I: system architecture and design of the driving situation identification process', *IEEE Trans. Veh. Technol.*, 2005, **54**, (3), pp. 925–934

28 Langari, R., Won, J.-S.: 'Intelligent energy management agent for a parallel hybrid vehicle – Part II: Torque distribution, charge sustenance strategies, and performance results', *IEEE Trans. Veh. Technol.*, 2005, **54**, (3), pp. 935–953

29 Montazeri, M., Asadi, M.: 'Intelligent approach for parallel HEV control strategy based on driving cycles', *International J. Syst. Sci.*, 2011, **42**, (2), pp. 287–302

30 Yushan, L., Qingliang, Z., Chenglong, W., Yuanjie, L.: 'Research on fuzzy logic control strategy for a plug-in hybrid electric city public bus'. Proc. Int. Conf. on Measuring Technol. and Mechatronics Automation, Changsha, China, March 2010, pp. 88–91

31 Li, S.G., Sharkh, S.M., Walsh, F.C., Zhang, C.N.: 'Energy and battery management of a plug-in series hybrid electric vehicle using fuzzy logic', *IEEE Trans. Veh. Technol.*, 2011, **60**, (8), pp. 3571–3585

32 Denis, N., Dubois, M.R., Gil, K.A., Driant, T., Desrochers, A.: 'Range prediction for a three-wheel plug-in hybrid electric vehicle'. Proc. ITEC, Dearborn, USA, June 2012, pp. 1–6

33 Tremblay, O., Dessaint, L., Dekkiche, A.: 'A generic battery model for the dynamic simulation of hybrid electric vehicles'. Proc. IEEE VPPC, Arlington, TX, USA, September 2007, pp. 284–289

34 Angarita Gil, K.P.: 'Modélisation Électrique et Analyse d'une Cellule Lithium'. Master's essay, Université de Sherbrooke, 2012

35 Gao, L., Liu, S., Dougal, R.A.: 'Dynamic lithium-ion battery model for system simulation', *IEEE Trans. Compon. Packag. Technol.*, 2002, **25**, (3), pp. 495–505

36 Hu, X., Li, S., Peng, H.: 'A comparative study of equivalent circuit models for Li-ion batteries', *J. Power Sources*, 2012, **198**, pp. 359–367

37 Lewis, F.L., Syrmos, V.L.: 'Dynamic programming', in (Eds.): 'Optimal control' (John Wiley & Sons, 1995, 2nd edn.), pp. 315–347